J. Electrochem. Sci. Eng. **14(2)** (2024) 147-161; http://dx.doi.org/10.5599/jese.2008

Open Access : : ISSN 1847-9286
www.jESE-online.org

Original scientific paper

Photo-bioelectrochemical cell anodes enhanced with titanium oxide, carbon nanotubes and chlorophyll-based catalyst on different supporting materials

Marcelinus Christwardana[1,2,✉], Athanasia Amanda Septevani[3,4] and Dilla Dayanti[2,3]

[1]*Department of Chemistry, Faculty of Science and Mathematics, Diponegoro University, Jl. Prof. Sudarto, S.H., Tembalang, Semarang 50275 , Indonesia*

[2]*Master Program of Energy, School of Postgraduate Studies, Diponegoro University, Jl. Imam Bardjo, S.H., Pleburan, Semarang50241, Indonesia*

[3]*Research Center for Environmental and Clean Technology, National Research and Innovation Agency, KST BRIN Cisitu, Bandung 40135, Indonesia*

[4]*Collaborative Researh Center for Zero Waste and Sustainability, Universitas Katolik Widya Mandala, Surabaya 60114, Indonesia*

Corresponding author: ✉marcelinus@lecturer.undip.ac.id

Received: July 31, 2023; Accepted: November 16, 2023; Published: December 11, 2023

Abstract

An important part of a photo-bioelectrochemical cell (PBEC) is the photo-biocatalyst substrate taken as anode. This study aims to explain the effect of CNT/TiO_2/chlorophyll photocatalyst coated on the cellulose nanopaper (CNP) substrate on the PBEC performance and to compare the results with those obtained for the commercial indium tin oxide (ITO) glass and flexible ITO as substrates. The results showed high sheet resistance of CNP, which is 61182 Ω sq^{-1}, which is reduced by 80 % in the presence of CNT/TiO_2/Chl biocatalyst. The highest output voltage of 0.95 to 1 V was produced by coating CNT/TiO_2/Chl on the flexible ITO. The maximum current density (J_{max}) of 3726 mA m^{-2} and the highest maximum power density value of around 574 mW m^{-2} were obtained for illuminated CNT/TiO_2/Chl on the rigid ITO anode. In dark conditions, the highest power density was observed for CNP as the supporting substrate. The photo-bioelectrochemical cell adopting CNT/TiO_2/Chl and CNP as the supporting substrate material has great potential for a variety of applications, such as wearable electronics, environmental monitoring, remote or off-grid energy supply, and renewable energy systems, thereby contributing to the advancement of sustainable energy technologies.

Keywords

Photo-bioanode; photo-biocatalyst substrates; flexible materials; natural dye catalyst; artificial photosynthesis; photo-current; maximum power density

Introduction

As a low-cost and eco-friendly alternative to conventional materials with excellent light harvesting efficiency, natural dyes have been the subject of intensive research in recent years [1,2]. This includes their use in photo-bioelectrochemical cells (PBECs) for the generation of electricity. Significant research efforts have been made to build semiconductor/photoelectrode hybrids for high-efficiency PBECs, which will help to bring sustainable solar energy to a commercially ready state [3,4]. For this reason, several natural pigments have been investigated as biocatalysts in PBECs systems [5]. Plant or microalgae pigments are able to do this because their electrical structure may alter the wavelength of incoming sunlight, creating an electric current [6,7]. This is due to the fact that photosynthesis may be performed by both land plants and microalgae.

Converting light energy into chemical energy in PBECs *via* photosynthesis is an efficient, sustainable, and complicated process [8,9]. Chlorophyll-rich thylakoid membranes and photo-systems from plants and microalgae are isolated and often employed as a source to convert light into electrical energy. Another crucial step in the creation of photo-current is the transit of electrons from the reaction center to the electrodes after their conversion from light [10,11]. Researchers have ramped up their efforts to create higher photo-currents by using natural and manmade components in the design of systems [12].

Previous research has shown that the photoanode of PBEC made up of a network of TiO_2 nanoparticles provides substantial specific surface area support sites for the adsorption of dye molecules [13]. To date, the highest reported relative photoconversion efficiency in PBECs has been achieved using TiO_2 [14]. However, the comparatively wide band gap of TiO_2 is a common deficiency of this material, which may be lowered by addition or alteration with a dye. The injected electrons tend to diffuse *via* trap-restricted diffusion processes across the matrix of random colloidal particles and grain boundaries of TiO_2 [15].

A substrate of photoanode is critical to PBECs as it serves as a support for the biocatalyst. Many solar cells rely on rigid substrates like ITO, but a flexible ITO was also employed in their development. Since the substrate is flexible, PBECs may be housed in a large variety of reactor geometries than possible with a rigid one. Rigid ITO is brittle and cracks easily during application, whereas flexible substrates can wear out over a long time. Rigid ITO costs more to produce since indium will be scarce in the future because it is a non-renewable material [16]. Flexible substrates can be bent or shaped according to the desired surface or shape, allowing solar cells to be fabricated on surfaces and shapes that rigid substrates cannot reach. Flexible substrates are typically lighter and slimmer than rigid substrates, reducing the weight and thickness of the whole PBEC. The use of flexible substrates can decrease the quantity of raw materials required to manufacture PBECs. Flexible substrates are typically more resistant to stress and vibration than rigid substrates that are brittle.

In this research, we describe the fabrication of a photo-biocatalyst composed of CNT, TiO_2, and chlorophyll coated on several substrates, including ITO glass, ITO flexible, and cellulose nano paper (CNP). The properties of CNP being produced on a lab scale will be compared to commercial ITO glass and flexible ITO. The hypothesis in this study is that the photo-biocatalyst coated on CNP has performance that is close to, or even better than, the photo-biocatalyst coated on either ITO glass or flexible ITO. Research on the influence of anode substrate on PBEC performance has never been conducted before. Hence, we consider this study to be an academic novelty. To assess the performance of PBECs, output voltage, current density, and power density will be evaluated. Some of the advantages and benefits resulting from this research include the development of innovative photo-biocatalysts, use of various supporting electrode materials, development of sustainable

materials, wide application such as water photocatalysis, pollutant detection, chlorophyll sensitive solar cells, as well as contribution to the environmental research and renewable energy.

Experimental

Catalyst fabrication

The extraction of chlorophyll from Spirulina is described in detail in the referenced articles [9,13]. In the first step, a commercial ITO glass (Hangzhou DCT Technology, Hangzhou, China), flexible ITO (Hangzhou DCT Technology, Hangzhou, China), and CNP [17] with dimensions of 1×1 cm were sonicated with ethanol medium for 15 minutes. The supporting materials were then placed on tissue paper and air-dried at room temperature. During the coating process, each edge of the supporting material was sealed to ensure that the catalyst paste was formed correctly in the center. Amounts of 0.25 g CNT (>95 % purity; 50 to 90 nm diameter) and 0.25 g TiO_2 (<100 nm; 99.5 % purity), purchased from Merck (Darmstadt, Germany), were mixed with 2 mL ethanol (95 %, commercial grade) during the catalyst coating preparation procedure. The liquid was combined until it formed a paste and poured over the isolated, four-sided support materials. On the surface of these supporting materials, catalyst paste was distributed consistently using a ruler. The prepared CNT/TiO_2 on supporting materials were then annealed for 15 minutes at 240 °C and washed using DI water to remove unbound CNTs. Then, these catalysts on support materials were left at room temperature (27 to 30 °C) for 2 hours. A 3 mL of chlorophyll (Chl) was dripped and left to stand for one day at room temperature. Before being used as a photo-bioanode, the CNT/TiO_2/Chl coating on the surface of the supporting material was washed with ethanol to remove unbound chlorophyll. Figure 1a illustrates the chemical pathway of forming the substrate coating using CNT, TiO_2, and chlorophyll. Figure 1b shows the image of a photo-bioanode with different supporting materials, while Figure 1c demonstrates the flexibility of CNT/TiO_2/Chl@CNP.

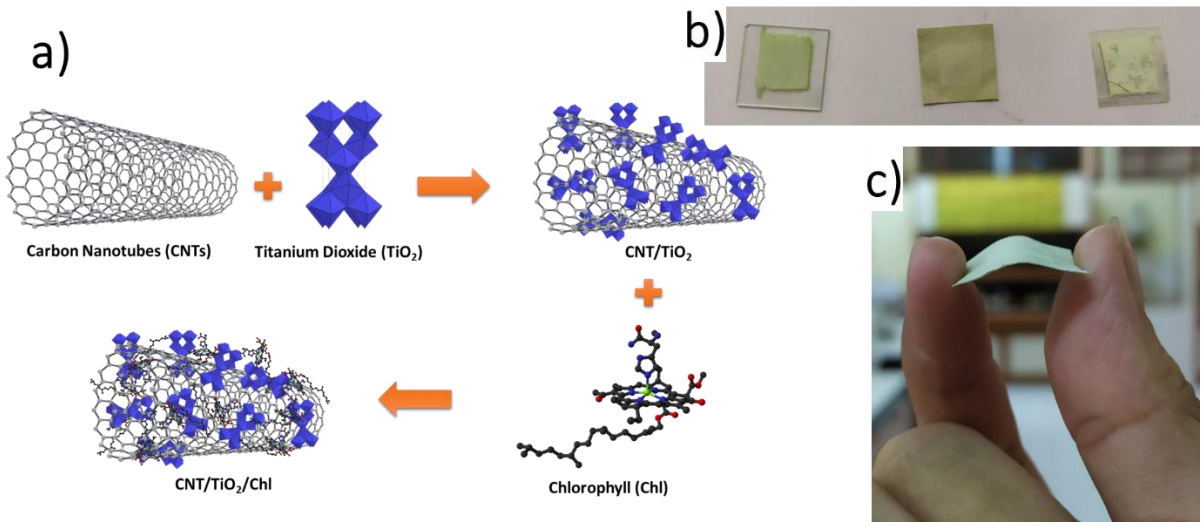

Figure 1. *a) Schematic of the synthesis of CNT/TiO_2/Chl deposited on b) ITO glass (left), cellulose nanopaper (middle), flexible ITO (right), and c) flexible cellulose nanopaper*

Reactor configuration

The scheme of PBEC is presented in Figure 2. The anode was composed of CNT/TiO_2/Chl bonded to supporting materials, while the cathode was composed of ITO/C placed at a distance of 5 cm from the anode. In the reaction chamber, the cathode transforms the oxygen released from the anode surface into water. A glass beaker served as the reaction cell, and the anode and cathode electrodes

were connected in series. For the purpose of this research, a photo-bioelectrochemical cell will use water as its electrolyte solution.

The photo-current tests were conducted using a customized solar simulator system, including a customized three-electrode electrochemical chamber, a customized light chamber equipped with a desk LED lamp (no brand) of changing light intensity and color temperature (2700 to 6000 K), and a digital light meter LX1010B to measure the actual light intensity within the chamber in real-time. The photo-bioelectrochemical system was then enclosed in a customized light chamber and sealed to prevent outside light from reaching it. This analysis is conducted twice, and the results shown are the mean.

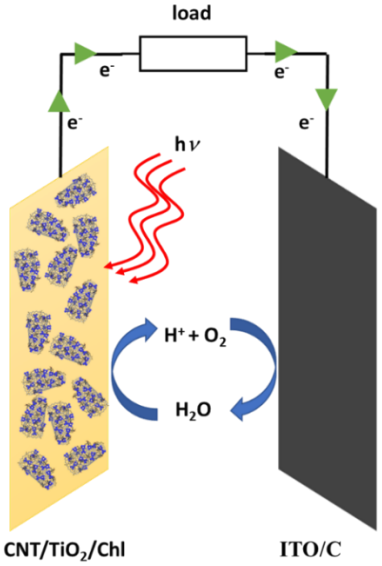

Figure 2. *Schematic diagram of photo-bioelectrochemical cell*

Electrochemical analysis

An Arduino-based potentiostat was connected to a computer to conduct electrochemical measurements, including half-cell and full-cell experiments. In half-cell measurements, the reference electrode was Ag/AgCl, and a Pt wire was employed as the counter electrode. The working electrode was a glassy carbon electrode (GCE) (Wuhan Corrtest Instruments Corp. Ltd., Hubei, China) with a diameter of 3.5 mm, on which the photo-biocatalyst was loaded. A small amount (10 µL) of photocatalyst ink with a concentration of 1 mg mL^{-1} was applied to the GCE surface and allowed to dry for 1 hour. The electrolyte solution used was 1 M PBS (pH 7.4) (Sigma Aldrich, St. Louis, USA), and the entire process was conducted under aerobic conditions without the addition of air gas.

To determine the open circuit voltage (OCV), the electrode of a photo-bioelectrochemical cell was methodically connected to a multimeter device (UNI-T UT-61E) without the addition of any external resistance. Then, the chronoamperometry (CA) measurement was established, and all CA readings were recorded using a multimeter in a light chamber with cyclic on/off illumination set at 1600 cd·sr m^{-2} (lux). Cell photo-current was measured at varying light illumination (900 to 1600 cd·sr m^{-2}) to determine light sensitivity. Polarization and power curves were determined at a closed-circuit voltage (CCV) using a range of resistor values from 10 MΩ to 100 Ω. Electric current was determined by dividing the measured voltage by the resistance of the load, power density was determined with the help of Ohm's law, and polarization curves were made using equations (1-3) [18]:

$$V = IR \quad (1)$$

$$J = I / A \quad (2)$$

$$P = VJ \quad (3)$$

where V / V is voltage, R / Ω is resistance, A / m^2 is electrode area, P / mW m^{-2} is power density, I / mA is current, and J / mA m^{-2} is current density.

FTIR and SEM analysis

FTIR (Perkin Elmer) instrument was used to examine the bond structures of the synthesized materials. The spectra were recorded from 4000 to 500 cm^{-1} at a spectra resolution of 4.0 cm^{-1}. A V-630 UV- VIS spectrometer (JASCO International Co., Japan) was used to record UV-Vis absorption spectra of synthesized samples from 300 to 800 nm. SEM-EDX JEOL JSM-6510LA (Tokyo, Japan) was used to inspect the morphology of the photo-biocatalyst.

Sheet resistance analysis

For measuring sheet resistance (R_s) of thin films, the four-point probe method is the most popular and straightforward approach [19]. In order to establish electrical contact with the material being characterized, a standard four-point probe instrument will typically include four equally spaced and co-linear probes. Applying a direct current (DC) through the outside probes causes a voltage to be induced between the two inner probes, which can then be used to determine the R_s. The sheet resistance may be determined by detecting this voltage drop using equation (4):

$$R_s = 4.53236\ \Delta V/I \quad (4)$$

where R_s / Ω sq^{-1} is the sheet resistance, ΔV is the voltage drop measured across the inner probes, and I is the current delivered at the outer probes.

Results and discussion

Physicochemical analysis

SEM analysis

Figure 3 depicts the SEM images of TiO_2, CNT/TiO_2, and CNT/TiO_2/Chl photo-biocatalysts. In the image of TiO_2 (Figure 3a), only agglomerated TiO2 is present. Van der Waals forces exist between individual TiO_2 particles, which helps form agglomerations by drawing together tiny particles [20].

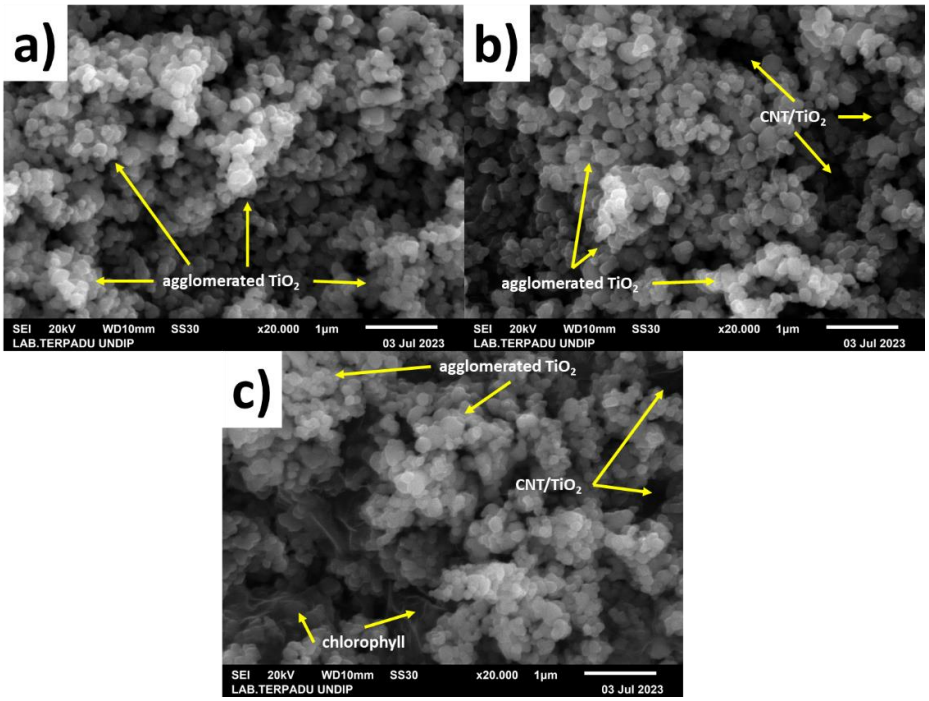

Figure 3. *SEM images of a) TiO_2, b) CNT/TiO_2, and c) CNT/TiO_2/Chl*

In CNT/TiO_2 image (Figure 3b), in addition to TiO_2 aggregates, there are also CNTs coated to TiO_2. Van der Waals forces can produce tangible connections between CNT and TiO_2. CNT and TiO_2 can also form hydrogen bonds, particularly through the oxygen atoms on TiO_2 and the hydrogen atoms affixed to the surface or extremities of CNT [21]. Due to the non-covalent nature of the interaction between CNTs and TiO_2, the binding strength is quite low. Consequently, it is hypothesized that a significant number of CNTs did not adhere to the TiO_2 surface and were subsequently removed during the washing procedure. Consequently, the observation of carbon nanotubes (CNTs) adhered to TiO_2 presents significant difficulties. In CNT/TiO_2/Chl image (Figure 3c), in addition to agglomerated TiO_2 and CNT/TiO_2/Chl, chlorophyll is also present, which was not the case with the previous photocatalyst. Chlorophyll contains numerous hydroxyl and carbonyl groups that can form hydrogen bonds with oxygen-rich CNT or TiO_2 molecules [13]. CNTs and the porphyrin ring in chlorophyll possess a plethora of π electrons. Interactions between the chlorophyll porphyrin ring and the carbon ring on the CNT or between two chlorophyll molecules can involve π-π stacking.

FTIR analysis

Figure 4 depicts the FTIR spectra of TiO_2, CNT/TiO_2, and CNT/TiO_2/Chl. These spectra disclose distinct characteristics of TiO_2, CNT/TiO_2, and CNT/TiO_2/Chl. A prominent peak at 1638 cm^{-1} in the CNT/TiO_2/Chl spectrum indicates the presence of representative C=C bonds between CNT and chlorophyll, an interaction not observed in the CNT/TiO_2 and TiO_2 spectra. The peak observed at 3354 cm^{-1} corresponds to the -OH bond, indicating an increase in intensity in CNT/TiO_2 and CNT/TiO_2/Chl, which suggests increased water absorption due to adsorption [22].

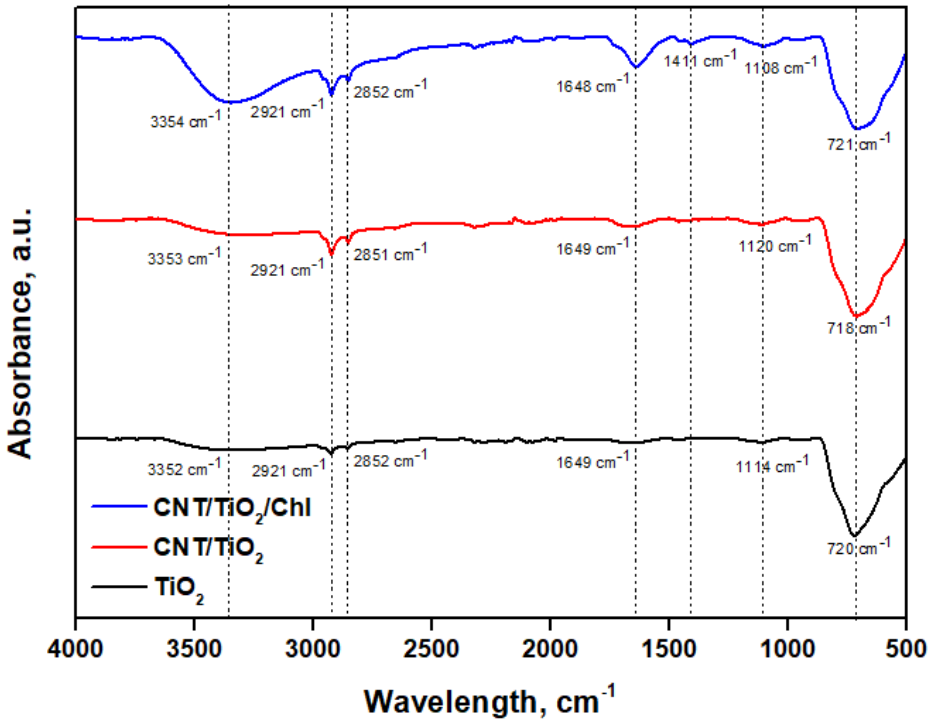

Figure 4. *FTIR spectra of TiO_2, CNT/TiO_2 and CNT/TiO_2/Chl*

The presence of peaks at 2851 and 2921 cm^{-1} provides additional support for this theory. A minor peak at 1649 cm^{-1} in CNT/TiO_2 is attributed to -N-O- bonds [23], whereas the peak at 1411 cm^{-1} in CNT/TiO_2/Chl represents CN stretching in chlorophyll [24,25]. In addition, a minor peak at 1108 to 1120 cm^{-1} indicates the presence of C-N-bonded or nitrogen oxide species [22]. According to Jiang *et al.* [26], the broad peak between 718 and 721 cm^{-1} corresponds to the O-Ti-O or Ti-O-Ti stretching

adsorption band in the TiO_2 lattice. These observations strongly suggest that chlorophyll binds strongly to the surface of CNT/TiO_2.

Half-cell characteristics

Cyclic voltammetry analysis

This study investigates the behavior and catalytic activity of PBEC anode structure made up of TiO_2, CNT/TiO_2 and CNT/TiO_2/Chl coated GC electrodes. Figure 5 shows CV profiles, which provide significant insight into the catalytic properties of the systems. Figure 5a highlights a number of observed phenomena. No redox peaks were observed in the GC, TiO_2, CNT/TiO_2, and CNT/TiO_2/Chl biocatalysts, suggesting the absence of any redox processes during the CV analysis. Furthermore, the introduction of TiO_2, CNT, and Chl to the GC results in a shifting of curves towards more negative current densities. This observation suggests that the presence of these materials promotes the oxygen reduction reaction (ORR), with the carbon-based electrode (GC and CNT) playing a more significant role in facilitating this reaction. Moreover, the specific capacitance value can be determined by assessing the area encompassed by the cyclic voltammetry curve. The specific capacitance values of GC, TiO_2, CNT/TiO_2, and CNT/TiO_2/Chl are 22.10, 23.30, 28.43, and 18.59 F g^{-1}, respectively.

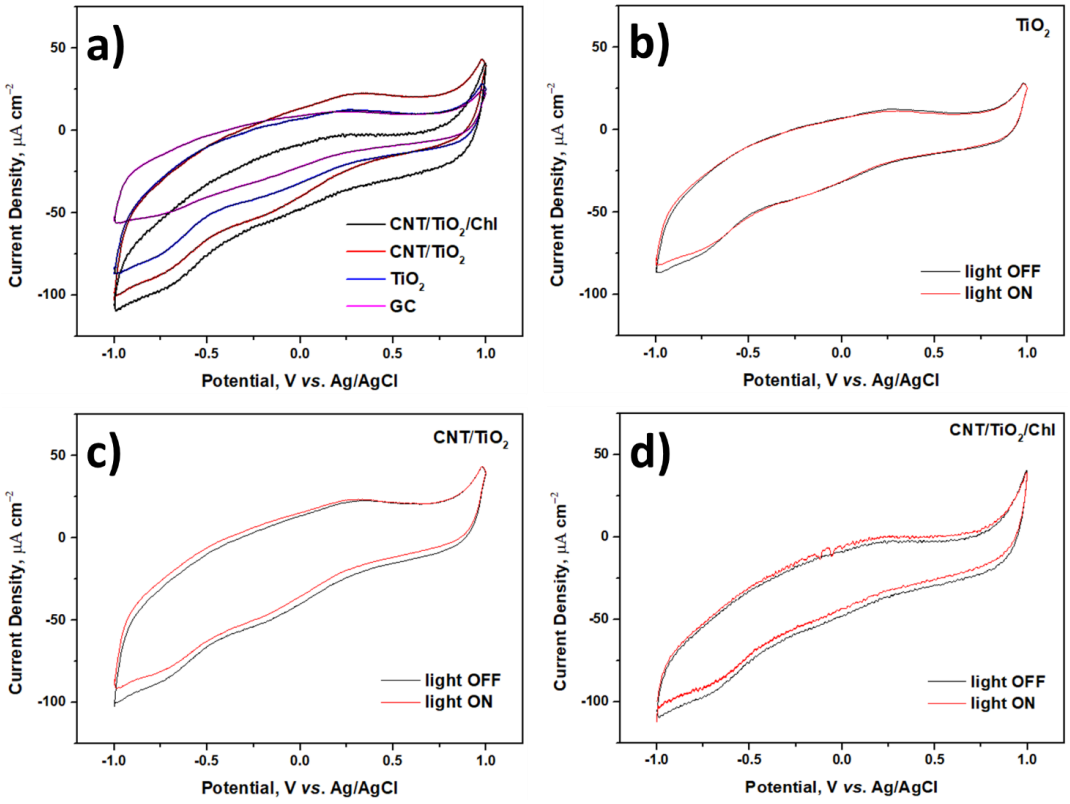

Figure 5. *a) CVs of GC, TiO_2, CNT/TiO_2 and CNT/TiO_2/Chl, and CVs with and without the presence of light for: b) TiO_2, c) CNT/TiO_2, and d) CNT/TiO_2/Chl*

Based on the specific capacitance findings, it can be concluded that CNT/TiO_2/Chl and TiO_2 exhibit favorable characteristics for utilization in energy conversion systems, such as PBEC, due to their comparatively lower specific capacitance values. In contrast, it is worth noting that the CNT/TiO_2 composite exhibits a comparatively higher specific capacitance, hence rendering it a more viable option for utilization in energy storage devices.

Due to their capacity to convert solar energy into electricity, PBEC systems are promising candidates for sustainable energy conversion, according to research findings. In these systems, the

anode catalyzes the oxidation of water molecules into oxygen and protons. TiO_2, an extensively used photocatalyst, has been shown to improve the charge transfer properties of the anode, thereby enhancing its catalytic activity. Due to their high surface area, electrical conductivity, and electrocatalytic properties, carbon nanotubes have also been used as catalysts in PBEC systems. The photosynthetic pigment chlorophyll increases the catalytic activity of the PBEC anode structure by facilitateing the transfer of electrons from the anode to the cathode. Overall, these findings suggest that PBEC systems have the potential to be efficient and environmentally friendly energy conversion solutions.

Figure 5b-d displays the CV curves of TiO_2, CNT/TiO_2, and CNT/TiO_2/Chl-coated GC electrodes in the presence or absence of light. In the presence of light, the CV curve of TiO_2 (Figure 4b) is at potentials less than -0.75 V *vs.* Ag/AgCl shifted marginally to less negative currents. Figures 5c and 5d demonstrate that this effect of less negative currents was also observed for CNT/TiO_2 and CNT/TiO_2/Chl. The presence of CNT on CNT/TiO_2 assists in the excitation of electrons when light is present and the transfer of electrons from the semiconductor material to the current collector, which also functions as a supporting material.

Sheet resistance of CNT/TiO_2/Chl at various supporting materials

Different substrates coated by CNT/TiO_2/Chl catalysts create different sheet resistances, where the type of supporting material has the strongest impact on the conductivity of the obtained materials (Figure 6). There are several points to consider. First, before being coated with CNT/TiO_2/Chl, the sheet resistance of CNP was 61182 Ω sq^{-1}, which is considerably higher in comparison to ITO glass and flexible ITO having sheet resistance values of 140 and 88 Ω sq^{-1}, respectively.

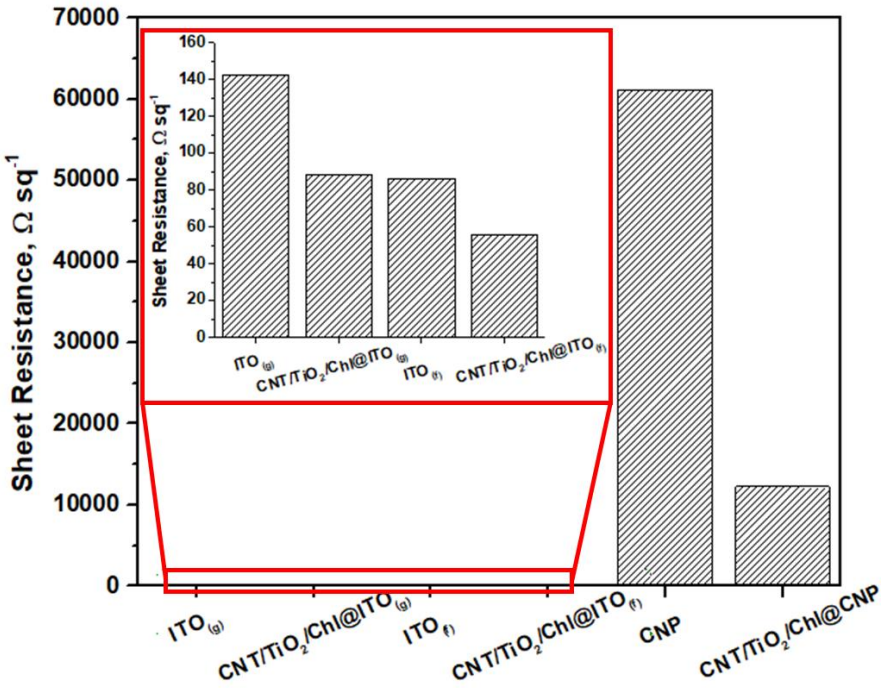

Figure 6. *Sheet resistance of $ITO_{(g)}$, $ITO_{(f)}$, CNP, CNT/TiO_2/Chl@$ITO_{(g)}$, CNT/TiO_2/Chl@$ITO_{(f)}$, and CNT/TiO_2/Chl@CNP*

This demonstrates that ITO is much more conductive than CNP. It is well known that ITO is a conductive substance and therefore, it may be employed as a supporting material for electrochemical cell electrodes [27]. Second, when CNT/TiO_2/Chl was coated on the surface of the supporting material, the sheet resistance was lowered, where CNT/TiO_2/Chl@CNP exhibited the greatest reduction (80 %). At the same time, the sheet resistances of ITO glass and flexible ITO

decreased by 38 and 35 %, respectively. This demonstrates that the CNT/TiO_2/Chl catalyst has excellent conductivity, allowing it to decrease the resistivity of the supporting material. This is the initial investment for use as the anode of a photo-bioelectrochemical cell in which the electrode must be conducting. According to the sheet resistance results, CNP as a supporting material for PBEC anodes is indeed much less conductive than ITO glass or flexible ITO, but CNP is more sustainable in terms of raw material production, and the coating of CNT/TiO_2/Chl catalysts is very good and very helpful for increasing the conductivity.

Full cell characteristics

The potential and photo-current density of photo-bioelectrochemical cell with different supporting materials

The effect of CNT/TiO_2/Chl coated on the surface of different supporting materials on bioelectrical power generation of built-up PBECs was investigated by varying the light intensity. As seen in Figure 7a, light/dark voltage and photo-current were created continuously and maintained for 50 minutes during a daily light/dark cycle for all tested light intensities. It was shown that the presence of chlorophyll in the biocatalyst structure generates energy with light intensities up to 1400 cd·sr m^{-2} (lux). Notably, there was a considerable rise in voltage when the light intensity was raised in the PBEC and a drop in voltage production when the light was turned off. All PBECs exhibited a fast rise in OCV upon exposure to light. However, the output voltage of the PBFC with CNT/TiO_2/Chl@$ITO_{(f)}$ anode was about 0.95 to 1 V, which is greater than for the same biocatalyst coated on $ITO_{(g)}$ and CNP, whose values were 0.84 to 0.85 and 0.8 to 0.83 V, respectively. As demonstrated in Figure 7b, upon illumination, the CNT/TiO_2/ /Chl at $ITO_{(g)}$, $ITO_{(f)}$, and CNP could create photo-current densities up to 3800, 2000 and 1500 mA m^{-2}, suggesting the higher photocurrent generated at $ITO_{(f)}$, than at $ITO_{(g)}$ and CNP. The sudden spike in photo-current is explained by the light intensity, and it was stabilized after 1-2 minutes. In particular, the photo-current density of CNT/TiO_2/Chl at $ITO_{(g)}$, $ITO_{(f)}$, and CNP in steady-state (stable) conditions are approaching 500, 730, and 620 mA m^{-2}, respectively. After turning off the light, the photo-current decreased.

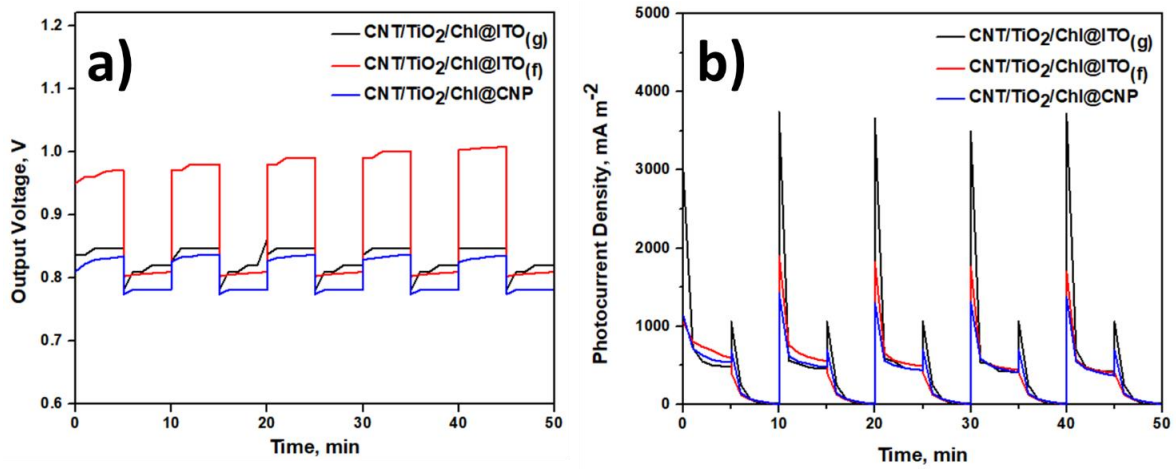

Figure 7. *a) Output voltage and b) photo-current density of CNT/TiO_2/Chl at different supporting materials with and without presence of light*

The conductivity of the biocatalyst and supporting materials of the anode, which influenced the electron transfer process, was responsible for the aforementioned findings. It is well established that reactive oxygen species (ROS) are generated during the photosynthetic process in the thylakoid membrane [28,29]. Damage to the reaction center proteins and their surroundings by reactive oxygen

species (ROSs) such as singlet oxygen ($^1O_2$), superoxide (O^{2-}), hydroxyl radicals (OH•), and hydrogen peroxide (H_2O_2) may slow down photosynthesis. These substances may also restrict the overall amount of electron transport by interfering with the path of electrons used to go from one place to another [30]. On the one hand, the conductivity of the supporting material and the biocatalyst, both of which enhance the transfer of electrons, may explain the superiority of the biocatalyst coated at ITO(f). However, poor conductivity would hinder the diffusional mass movement of electrons, a slow kinetic process that is likely rate-limiting for electron transfer inside a biocatalyst-modified electrode.

Sensitivity of photo-bioelectrochemical cell

PBEC performance might indicate the sensitivity between biocatalyst and light as fuel, making it crucial to investigate how light intensity affects the electrical current generated by these cells. Michaelis-Menten is a mathematical model used in biochemistry and pharmacology to describe the kinetics of enzymes (biocatalysts) with organic materials (fuel). For PBEC, Michaelis-Menten can be adapted since chlorophyll acts as a biocatalyst and light acts as a fuel, even though it is "apparent" fuel. Meanwhile, maximum current density (J_{max}) in PBEC is the maximum photo-current density that can be produced when the light illumination is unlimited. The Michaelis-Menten formula adopted in the photo-biocatalyst application can be written as in equation (5):

$$J_0 = \frac{J_{max} E_v}{K_m E_v} \tag{5}$$

where J_0 and J_{max} are initial and maximum current density, K_m is the Michaelis-Menten constant, and E_v is light illumination. The apparent Michaelis–Menten constant (K_m), J_{max}, and light sensitivity were also measured, as shown in Figure 8 [31].

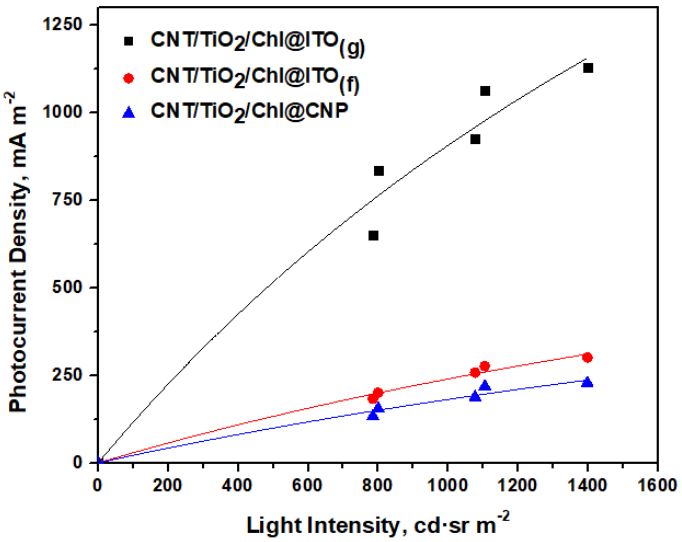

Figure 8. *Michaelis-Menten plot of CNT/TiO_2/Chl at different supporting materials with various light intensities*

The K_m and J_{max} values of CNT/TiO_2/Chl at $ITO_{(g)}$, $ITO_{(f)}$, and CNP were 3106, 4040 and 4564 cd·sr m^{-2} and 3726, 1209, and 1009 mA m^{-2}, respectively. When the K_m value is less, the catalyst of the photo-bioanode is more responsive to light [13]. Each curve slope was measured to confirm the sensitivity. CNT/TiO_2/Chl@$ITO_{(g)}$ continues to have the highest sensitivity among the three samples with 1.199 mA cd·sr m^{-4} (mA m^{-2} lx^{-1}), followed by CNT/TiO_2/Chl@$ITO_{(f)}$ with 0.299 mA cd·sr m^{-4} and CNT/TiO_2/Chl@CNP with 0.221 mA cd·sr m^{-4}. According to the data shown above, the CNT/TiO_2/ /Chl@$ITO_{(g)}$ sample is the most light-responsive among the three investigated samples.

Analysis of polarization and power curves of photo-bioelectrochemical cell

The performance of the PBEC was further tested by subjecting it to discharge tests using various external resistances. As can be seen in Figure 9a, CNT/TiO_2/Chl@$ITO_{(g)}$ applied as the anode produced the highest power density under illumination, at roughly 574 mW m^{-2}, followed by CNT/TiO_2/Chl@CNP at 247 mW m^{-2}, or 60 % lower. The lowest maximum power density of 140 mW m^{-2} was achieved with CNT/TiO_2/Chl@$ITO_{(f)}$. The CNT/TiO_2/Chl coated on the surface of $ITO_{(f)}$, $ITO_{(g)}$, and CNP were all examined for their ability to generate power in the dark (Figure 9b), with obtained maximum power density values of 81, 107, and 122 mW m^{-2}. This is due to the following reasons: (i) conductive anode supporting materials, (ii) the presence of CNT/TiO_2/Chl biocatalyst that, due to its conductivity and active surface area, can increase the rate at which electrons are transferred, increasing thus the maximum power density, and (iii) CNP is better able to store energy. Hence it has more capacitance-related properties than conductance-related ones. Concerning the biological process, chlorophyll performed admirably in converting H_2O into H^+, electrons (e^-), and oxygen (O_2). Because of the interaction between the dye molecules and TiO_2 molecules, electrons may be transferred from the excited dye molecules to the TiO_2 layer, resulting in increased energy production [32]. In a PBEC, adding oxygen gas may maximize the oxygen reduction reaction (ORR) on the cathode side. The efficiency of the cells is dependent on the electrode material, the usage of membrane separators, and the cell system or design, much as in enzymatic or microbial fuel cells. The production costs of electrodes made using precious metals (gold or platinum) are higher than those made from non-metals. This also includes the creation of sophisticated electrode byproducts. Complex synthesis procedures lead to greater manufacturing costs; thus, marketing should be prioritized accordingly.

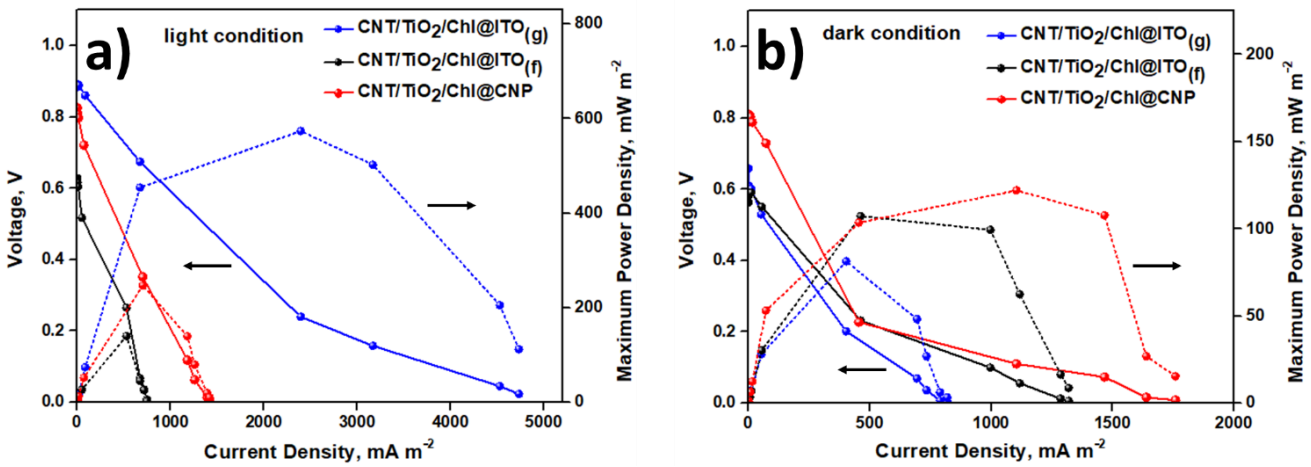

Figure 9. *Polarization (solid lines) and power curves (dotted lines) of photo-bioelectrochemical cell adopting CNT/TiO_2/Chl on different supporting materials in a) light and b) dark conditions*

Future prospects of TiO_2/CNT/Chl as the anode catalyst of flexible photo-bioelectrochemical cell

Flexible PBEC with CNT/TiO_2/Chl as the anode photocatalyst at the cellulose nanopaper (CNP) as the supporting substrate material is very promising for various applications. In the field of wearable electronics, these cells could be incorporated into garments or accessories to power devices like fitness monitors, medical sensors, and wearables. This provides a renewable and self-sufficient energy source for such devices. Another potential use is in environmental monitoring. This flexible and environmentally friendly cell can serve as a sensor for monitoring parameters like water quality, air pollution, and soil health. They could be deployed in remote or inaccessible areas to provide real-

time environmental data for assessment and management. These cells are also suitable for powering small-scale electronic devices in remote or off-grid locations with limited access to conventional energy sources, such as communication systems, illumination, or sensors, offering a source of sustainable energy. The scalability and cost-effectiveness of manufacturing processes for these cells make them suitable for widespread application in renewable energy systems. They can be integrated into building facades, ceilings, or windows to harness solar energy and generate on-site electricity, contributing to green buildings and sustainable urban environments.

Conclusions

This comprehensive study investigates the performance of PBECs utilizing a novel anode catalyst, CNT/TiO_2/Chl, coated on different supporting materials. The research encompasses a rigorous analysis of physicochemical properties, cyclic voltammetry, sensitivity assessments, and power generation capabilities, providing valuable quantitative results. Physicochemical analyses, such as SEM and FTIR, elucidate the structural composition of the catalysts. The SEM images reveal the successful incorporation of chlorophyll, while FTIR spectra demonstrate distinctive characteristics, including the presence of C=C bonds and -OH bonds. Quantitatively, the specific capacitance values of GC, TiO_2, CNT/TiO_2, and CNT/TiO_2/Chl are determined as 22.10, 23.30, 28.43, and 18.59 F g^{-1}, respectively, indicating the favorable characteristics of CNT/TiO_2/Chl and TiO_2 for energy conversion. Cyclic voltammetry profiles uncover the catalytic activity, with the electrical double layer current densities shifting towards more negative values upon the introduction of TiO_2, CNT, and Chl due to the contribution of ORR reaction. Specific capacitance values further confirm the superior performance of CNT/TiO_2, particularly in energy storage applications. Quantitatively, the photocurrent densities of CNT/TiO_2/Chl at $ITO_{(g)}$, $ITO_{(f)}$, and CNP in steady-state conditions approach 500, 730, and 620 mW m^{-2}, respectively. The study explores the sensitivity of PBECs, employing a mathematical model adapted from Michaelis-Menten kinetics. Quantitative results include K_m and J_{max} values for CNT/TiO_2/Chl at $ITO_{(g)}$, $ITO_{(f)}$, and CNP, revealing the biocatalyst light responsiveness. Full cell characteristics unveil the quantitative power generation capabilities of PBECs. Under illumination, CNT/TiO_2/Chl@$ITO_{(g)}$ produces the highest power density at approximately 574 mW m^{-2}, followed by CNT/TiO_2/Chl@CNP at 247 mW m^{-2}. In the dark, maximum power density values of 81, 107, and 122 mW m^{-2} are observed for CNT/TiO_2/Chl at $ITO_{(g)}$, $ITO_{(f)}$, and CNP, respectively. Quantitative results from polarization and power curves affirm the superior performance of CNT/TiO_2/Chl@$ITO_{(g)}$ in power generation, with a maximum power density of approximately 574 mW m^{-2} under illumination.

In conclusion, the quantitative data substantiates the efficacy of the CNP as supporting material, positioning it as a robust candidate to substitute existing ITO glass or flexible ITO as supporting material of PBECs when CNT/TiO_2/Chl acted as photo-biocatalyst. Its superior capacitance, light responsiveness, and power generation capabilities, coupled with flexibility and environmental compatibility, underscore its potential for diverse applications in sustainable energy solutions. These flexible photo-bioelectrochemical cells hold great promise in the realm of sustainable energy technologies. Their ability to efficiently convert solar energy into electricity, as demonstrated in our research, underscores their potential significance in advancing sustainable energy solutions.

Acknowledgements*: This research was supported in full with Toray Science & Technology Research Grant 2020 provided by Indonesia Toray Science Foundation.*

References

[1] N. Mariotti, M. Bonomo, L. Fagiolari, N. Barbero, C. Gerbaldi, F. Bella, C. Barolo, Recent advances in eco-friendly and cost-effective materials towards sustainable dye-sensitized solar cells, *Green Chemistry* **22** (2020) 7168-7218. https://doi.org/10.1039/D0GC01148G

[2] P. Semalti, S. N. Sharma, Dye sensitized solar cells (DSSCs) electrolytes and natural photo-sensitizers: a review, *Journal of Nanoscience and Nanotechnology* **20** (2020) 3647-3658. https://doi.org/10.1166/jnn.2020.17530

[3] C. M. Hanna, R. T. Pekarek, E. M. Miller, J. Y. Yang, N. R. Neale, Decoupling Kinetics and Thermodynamics of Interfacial Catalysis at a Chemically Modified Black Silicon Semiconductor Photoelectrode, *ACS Energy Letters* **5** (2020) 1848-1855. https://doi.org/10.1021/acsenergylett.0c00714

[4] F. Niu, D. Wang, F. Li, Y. Liu, S. Shen, T. J. Meyer, Hybrid photoelectrochemical water splitting systems: from interface design to system assembly, *Advanced Energy Materials* **10** (2020) 1900399. https://doi.org/10.1002/aenm.201900399

[5] E. Musazade, R. Voloshin, N. Brady, J. Mondal, S. Atashova, S. K. Zharmukhamedov, I. Huseynova, S. Ramakrishna, M. M. Najafpour, J.-R. Shen, B. D. Bruce, S. I. Allakhverdiev, Biohybrid solar cells: Fundamentals, progress, and challenges, *Journal of Photochemistry and Photobiology C: Photochemistry Reviews* **35** (2018) 134-156. https://doi.org/10.1016/j.jphotochemrev.2018.04.001

[6] A. Orona-Navar, I. Aguilar-Hernández, T. López-Luke, A. Pacheco, N. Ornelas-Soto, Dye sensitized solar cell (DSSC) by using a natural pigment from microalgae, *International Journal of Chemical Engineering and Applications* **11** (2020) 14-17. https://doi.org/10.18178/ijcea.2020.11.1.772

[7] N. T. R. N. Kumara, A. Lim, C. M. Lim, M. I. Petra, P. Ekanayake, Recent progress and utilization of natural pigments in dye sensitized solar cells: A review, *Renewable and Sustainable Energy Reviews* **78** (2017) 301-317. https://doi.org/10.1016/j.rser.2017.04.075

[8] A. Efrati, C. H. Lu, D. Michaeli, R. Nechushtai, S. Alsaoub, W. Schuhmann, I. Willner, Assembly of photo-bioelectrochemical cells using photosystem I-functionalized electrodes, *Nature Energy* **1** (2016) 15021. https://doi.org/10.1038/nenergy.2015.21

[9] M. Christwardana, A. A. Septevani, L. A. Yoshi, Sustainable electricity generation from photo-bioelectrochemical cell based on carbon nanotubes and chlorophyll anode, *Solar Energy* **227** (2021) 217-223. https://doi.org/10.1016/j.solener.2021.09.002

[10] V. Mascoli, A. F. Bhatti, L. Bersanini, H. van Amerongen, R. Croce, The antenna of far-red absorbing cyanobacteria increases both absorption and quantum efficiency of Photosystem II, *Nature Communications* **13** (2022) 3562. https://doi.org/10.1038/s41467-022-31099-5

[11] M. Li, V. Svoboda, G. Davis, D. Kramer, H. H. Kunz, H. Kirchhoff, Impact of ion fluxes across thylakoid membranes on photosynthetic electron transport and photoprotection, *Nature Plants* **7** (2021) 979-988. https://doi.org/10.1038/s41477-021-00947-5

[12] Y. S. Chang, H. C. Yang, L. Chao, Formation of Supported Thylakoid Membrane Bioanodes for Effective Electron Transfer and Stable Photo-current, *ACS Applied Materials & Interfaces* **14** (2022) 22216-22224. https://doi.org/10.1021/acsami.2c04764

[13] M. Christwardana, A. A. Septevani, L. A. Yoshi, Outstanding Photo-bioelectrochemical Cell by Integrating TiO_2 and Chlorophyll as Photo-bioanode for Sustainable Energy Generation, *International Journal of Renewable Energy Development* **11** (2022) 385. https://doi.org/10.14710/ijred.2022.41722

[14] D. Kim, A. Ghicov, P. Schmuki, TiO_2 Nanotube arrays: Elimination of disordered top layers ("nanograss") for improved photoconversion efficiency in dye-sensitized solar cells, *Electrochemistry Communications* **10** (2008) 1835-1838. https://doi.org/10.1016/j.elecom.2008.09.029

[15] W. Hou, R. Hu, S. Zhu, Y. Xiao, G. Han, A thiourea resin polymer as a multifunctional modifier of the buried interface for efficient perovskite solar cells with reduced lead leakage, *Materials Chemistry Frontiers* **6** (2022) 3338-3348. https://doi.org/10.1039/D2QM00703G
[16] S. Lu, Y. Sun, K. Ren, K. Liu, Z. Wang, S. Qu, Recent development in ITO-free flexible polymer solar cells, *Polymers* **10** (2017) 5. https://doi.org/10.3390/polym10010005
[17] A. K. Prabowo, A. P. Tiarasukma, M. Christwardana, D. Ariyanti, Microbial Fuel Cells for Simultaneous Electricity Generation and Organic Degradation from Slaughterhouse Wastewater, *International Journal of Renewable Energy Development* **5** (2016) 107-112. http://dx.doi.org/10.14710/ijred.5.2.107-112
[18] A. A., Septevani, D., Burhani, Y., Sampora, Indriyati, Shobih, E. S., Rosa, D. Sondari, N. I. Margyaningsih, M. Septiyani, F. Yurid, & A. S. Handayani, A systematic study on the fabrication of transparent nanopaper based on controlled cellulose nanostructure from oil palm empty fruit bunch, *Journal of Polymers and the Environment* **30** (2022) 3901-3913. https://doi.org/10.1007/s10924-022-02484-4
[19] J. H. Lee, S. H. Kang, H. Ruh, K. M. Yu, Development of a thickness meter for conductive thin films using four-point probe method, *Journal of Electrical Engineering & Technology* **16** (2021) 2265-2273. https://doi.org/10.1007/s42835-021-00725-5
[20] Z. E. Allouni, M. R. Cimpan, P. J. Høl, T. Skodvin, N. R. Gjerdet, Agglomeration and sedimentation of TiO_2 nanoparticles in cell culture medium, *Colloids and Surfaces B: Biointerfaces* **68** (2009) 83-87. https://doi.org/10.1016/j.colsurfb.2008.09.014
[21] S. M. Miranda, G. E. Romanos, V. Likodimos, R. R. Marques, E. P. Favvas, F. K. Katsaros, K. L. Stefanopoulos, V. J. P. Vilar, J. L. Faria, P. Falaras, A. M. T. Silva, Pore structure, interface properties and photocatalytic efficiency of hydration/dehydration derived TiO_2/CNT composites, *Applied Catalysis B: Environmental*, **147** (2014) 65-81. https://doi.org/10.1016/j.apcatb.2013.08.013
[22] L., Lv, K., Li, Y., Xie, Y., Cao, X. Zheng, Enhanced osteogenic activity of anatase TiO_2 film: Surface hydroxyl groups induce conformational changes in fibronectin, *Materials Science and Engineering: C* **78** (2017) 96-104. https://doi.org/10.1016/j.msec.2017.04.056
[23] G. Huang, T. W. Ng, T. An, G. Li, B. Wang, D. Wu, H. Y. Yip, H. Zhao, P. K. Wong, Interaction between bacterial cell membranes and nano-TiO_2 revealed by two-dimensional FTIR correlation spectroscopy using bacterial ghost as a model cell envelope, *Water Research* **118** (2017) 104-113. https://doi.org/10.1016/j.watres.2017.04.023
[24] W. A. Dhafina, M. Z. Daud, H. Salleh, The sensitization effect of anthocyanin and chlorophyll dyes on optical and photovoltaic properties of zinc oxide based dye-sensitized solar cells, *Optik* **207** (2020) 163808. https://doi.org/10.1016/j.ijleo.2019.163808
[25] H. Nan, H. P. Shen, G. Wang, S. D. Xie, G. J. Yang, H. Lin, Studies on the optical and photoelectric properties of anthocyanin and chlorophyll as natural co-sensitizers in dye sensitized solar cell, *Optical Materials* **73** (2017) 172-178. https://doi.org/10.1016/j.optmat.2017.07.036
[26] D. Jiang, Y. Xu, D. Wu, Y. Sun, Visible-light responsive dye-modified TiO_2 photocatalyst, *Journal of Solid State Chemistry* **181** (2008) 593-602. https://doi.org/10.1016/j.jssc.2008.01.004
[27] Z. Karami, A. Soleimani-Gorgan, G. R. Vakili-Nezhaad, F. A. Roghabadi, A layer-by-layer green inkjet printing methodology for developing indium tin oxide (ITO)-based transparent and conductive nanofilms, *Journal of Cleaner Production* **379** (2022) 134455. https://doi.org/10.1016/j.jclepro.2022.134455
[28] D. V. Vetoshkina, M. M. Borisova-Mubarakshina, I. A. Naydov, M. A. Kozuleva, B. N. Ivanov, Impact of high light on reactive oxygen species production within photosynthetic biological

membranes, *Journal of Biology and Life Science* **6** (2015) 50-60. http://dx.doi.org/10.5296/jbls.v6i2.7277

[29] A. Krieger-Liszkay, G. Shimakawa, Regulation of the generation of reactive oxygen species during photosynthetic electron transport, *Biochemical Society Transactions* **50** (2022) 1025-1034. https://doi.org/10.1042/BST20211246

[30] G. Lenaz, Mitochondria and reactive oxygen species. Which role in physiology and pathology?, *Advances in Mitochondrial Medicine* (2012) 93-136. https://doi.org/10.1007/978-94-007-2869-1_5

[31] M. Christwardana, Combination of physico-chemical entrapment and crosslinking of low activity laccase-based biocathode on carboxylated carbon nanotube for increasing biofuel cell performance, *Enzyme and Microbial Technology* **106** (2017) 1-10. https://doi.org/10.1016/j.enzmictec.2017.06.012

[32] A. Boyo, O. Paul, I. Abdulsalami, O. Surukite, H. O. Boyo, H. Boyo, Application of Hibiscus sabdariffa and leaves of Azardirachta indica calyxes as sensitizers in dye-sensitized solar cells, *International Journal of Engineering Research and Development* **8** (2013) 38-42. https://www.ijerd.com/paper/vol8-issue12/F08123842.pdf